Liquid Crystals

Publication details, including instructions for authors and subscription information:
http://www.informaworld.com/smpp/title~content=t713926090

Synthesis and mesomorphic behaviour of novel chiral nematic side chain liquid crystalline polysiloxanes

Bao-yan Zhang Corresponding author; Jun-ge Zhi; Fan-bao Meng

To cite this Article Zhang Corresponding author, Bao-yan , Zhi, Jun-ge and Meng, Fan-bao(2003) 'Synthesis and mesomorphic behaviour of novel chiral nematic side chain liquid crystalline polysiloxanes', Liquid Crystals, 30: 9, 1007 — 1014

To link to this Article: DOI: 10.1080/0267829031000010712

URL: http://dx.doi.org/10.1080/0267829031000010712

PLEASE SCROLL DOWN FOR ARTICLE

LIQUID CRYSTALS, VOL. 30, NO. 9, SEPTEMBER, 2003, 1007–1014

Taylor & Francis
Taylor & Francis Group

Synthesis and mesomorphic behaviour of novel chiral nematic side chain liquid crystalline polysiloxanes

BAO-YAN ZHANG*, JUN-GE ZHI and FAN-BAO MENG
Centre for Molecular Science and Engineering, Northeastern University,
Shen-Yang 110004, PR China

(*Received 12 August 2002; in final form 30 January 2003; accepted 20 February 2003*)

A series of novel thermotropic side chain liquid crystalline polymers was synthesized by grafting copolymerization of a mesogenic monomer, 4-allyloxybenzoyl-4′ -(4-*n*-alkylbenzoyl)–*p*-benzenediol bisate and a chiral monomer, menthyl undecylenate. The mesogenic monomers exhibited nematic threadlike textures during heating and cooling. The polymers showed thermotropic liquid crystalline properties with a broad mesomorphic region over a range of 100°C. The polymers exhibited a cholesteric mesophase with a colourful Grand-Jean texture when the content of chiral units was greater than 15 mol%; the others exhibited nematic threadlike textures. All of the polymers were thermally stable over 300°C, and most were laevorotatory as the chiral monomer.

1. Introduction

Thermotropic liquid crystalline polymers (LCPs) are an important class of high performance materials that provide good thermal stability, excellent chemical resistance, and outstanding mechanical properties [1, 2]. The discovery of ferroelectricity in a chiral smectic liquid crystal by Meyer [3] has attracted much interest in chiral liquid crystalline polymers. Because the chiral molecules can give rise to superstructures in which the local dielectric tensor rotates in space producing a helix [4, 5], chiral LC polymers exhibit unique optical properties such as selective light reflection, optical rotation and circular dichroism. These properties form the basis of a number of potential optoelectronic applications, including optical data storage materials, circular polarizers, and a high efficiency LC color display and projection system [6]. Chiral side chain LCPs can be obtained by the combination of a mesogenic unit and a chiral component, or by polymerization of chiral mesogenic units [7, 8]. The structure of the mesogneic unit, the properties of the chiral unit, and the flexibility and nature of the polymer backbone will influence the LC properties and orientation states of chiral side chain LCPs.

Siloxane polymers are materials of significant technological interest. The siloxane bond offers a highly flexible structural unit, yielding polymer chains with low glass transition temperatures, low surface tensions and unique physical and chemical properties [9]. In previous studies, we reported the synthesis and properties of a series of chiral side chain LC polysiloxanes with sulphonate ionic groups [10] and a series of photochromic side chain cholesteric LC polysiloxanes [11]. In this article, we report the synthesis of a series of chiral side chain LC polymers containing a nematic monomer possessing a broad mesogenic phase, and a chiral non-mesogenic monomer, menthyl undecylenate, which is laevorotatory with a specially high rotation. The thermotropic LC properties, anisotropic textures and chiroptical properties of the monomers and polymers are discussed.

2. Experimental

2.1. *Materials*

Polymethylhydrosiloxane (PMHS, $M_n = 700–800$) was obtained from Jilin Chemical Industry Company (China). Toluene was distilled after drying over $CaCl_2$ for 48 h. Tetrahydrofuran (THF) was dried with molecular sieves, heated under reflux over lithium hydride and then distilled. Allyl bromide was distilled before use.

2.2. *Characterization*

IR spectra were recorded using a Nicolet 510P FTIR spectrometer (Nicolet Instruments, Madison, WI) as KBr pellets. Thermal transition temperatures were determined with a Perkin-Elmer DSC-7 (Perkin-Elmer, Foster City, CA) equipped with a liquid nitrogen cooling system at a heating rate of 20°C min^{-1} in a

*Author for correspondence;
e-mail: baoyanzhang@hotmail.com

Liquid Crystals ISSN 0267-8292 print/ISSN 1366-5855 online © 2003 Taylor & Francis Ltd
http://www.tandf.co.uk/journals
DOI: 10.1080/0267829031000010712

nitrogen atmosphere. The reported thermal transitions were collected during the second heating and cooling scans. A Leitz Microphot-FX (Leitz, Wetzlar, Germany) polarizing optical microscope (POM) equipped with a Mettler FP82 hot stage and an FP 80 central processor was used to observe the thermal transitions and analyse the anisotropic textures. X-ray diffraction (XRD) measurements were performed with nickel-filtered Cu-K$_\alpha$ radiation using a Rigaku powder diffractrometer. Measurement of chiroptical rotation was carried out with a Shanghai WZZ-1S digital polarimeter (Shanghai, China) using toluene as solvent.

2.3. *Synthesis of mesomorphic monomers 4-allyloxybenzoyl-4′-(4-n-alkylbenzoyl)–p-benzenediol bisate (M1, M2, M3)*

4-Hydroxyphenyl 4-allyloxybenzoate was synthesized according to a literature procedure [10].

The syntheses of the 4-allyloxybenzoyl-4′-(4-*n*-alkylbenzoyl)–*p*-benzenediol bisate were identical; the synthesis of monomer M1 is given as an example (see the scheme).

In a 250 ml flask, 4-methylbenzoyl chloride (0.22 mol) was added dropwise to a 150 ml THF solution containing 4-hydroxyphenyl 4-allyloxybenzoate (0.2 mol) and a catalytic amount of pyridine (1 ml). The mixture was stirred at 60–65°C for 6 h and poured into water. The precipitate obtained was washed with 0.5M NaOH aqueous solution (200 ml) and water (1000 ml), and recrystallized from ethanol. White crystals were obtained. The yield and melting points of monomers M1, M2, M3 are summarized in table 1. IR (KBr): 2850–2980 cm^{-1} (CH_3–, –CH_2–), 1732 cm^{-1} (C=O), 1604–1450 cm^{-1} (⌬), 1250 cm^{-1} (C–O).

2.4. *Synthesis of chiral monomer menthyl undecylenate (Mc)*

Menthyl undecylenate (Mc) was synthesized according to a literature procedure [12]. Yield 85%, $[\alpha]_D^{15} = -41.3°$. IR (KBr): 3032 cm^{-1} (=C–H), 2873, 2930 cm^{-1} (CH_3–, –CH_2–), 1735 cm^{-1} (C=O), 1635 cm^{-1} (C=C).

2.5. *Synthesis of polymers*

The polymer synthesis is outlined in the scheme, and the monomer compositions used in polymerization are summarized in table 2. For the synthesis of polymers P1, the monomers M1, Mc and PMHS were dissolved in dry freshly distilled toluene. A hexachloroplatinic acid/THF solution was added under nitrogen, the molar ratio of Pt/alkene being 1/10^3. The reaction temperature was 60–65°C, and the reaction process was followed by monitoring the disappearance of the Si–H stretch at 2160 cm^{-1} using FTIR spectroscopy. Upon completion of the reaction, the products were separated by precipitation into an excess of methanol. The products were washed with methanol repeatedly, then dried in a vacuum oven at room temperature.

3. Results and discussion

3.1. *Chiroptical properties*

The monomer Mc and most of the polymers P1, P2, P3 in toluene solution were optically active at 589 nm, analogous to other copolymers [13, 14]. The specific rotatory power (SRP) of chiral monomer Mc was −41.3°, and the SRPs of the polymers showed similar negative values to Mc when the chiral Mc content was higher than 10 mol%; this indicated that the polymers are levorotatory, as shown in table 2. The Mc SRP value was higher than those of the polymers. The SRPs of polymers P1 and P2 increased linearly depending on the Mc content, while an approximately linear dependence of SRP on Mc content was observed for P3 at the sodium D line. The variation of SRP for P1, P2 and P3 with the Mc content is shown in figure 1. This variation was consistent with the expression $-[\alpha]_D^{15} = 20c + 2$ (where c is the mol% of chiral monomer Mc). The higher SRP of Mc and the increase of SRP with increasing Mc content may be explained by the van't Hoff Optical Rotation Addition Theory [15]. The SRP of an optically active compound is the total contribution of every chiral molecule. The concentration of optically active centre per mass of polymer sample was lower than that of Mc alone, thus the SRP of Mc was higher. The SRP increase is attributed to the increase in

Table 1. Yields and phase transition temperatures of monomers M1–M3.

			Second heating/°C			First cooling/°C			
Monomer	n	Yield/%	T_m	T_i	ΔT^a	T_c	T_{cr}	$\Delta T'^a$	Mesophase
M1	1	87	142.9	247.3	104.4	238.6	124.7	113.9	N^b
M2	3	85	136.4	239.5	103.1	222.5	104.4	118.1	N^b
M3	5	89	107.6	223.7	116.1	207.8	85.8	122.0	N^b

[a] ΔT is the mesomorphic temperature range.

[b] Nematic.

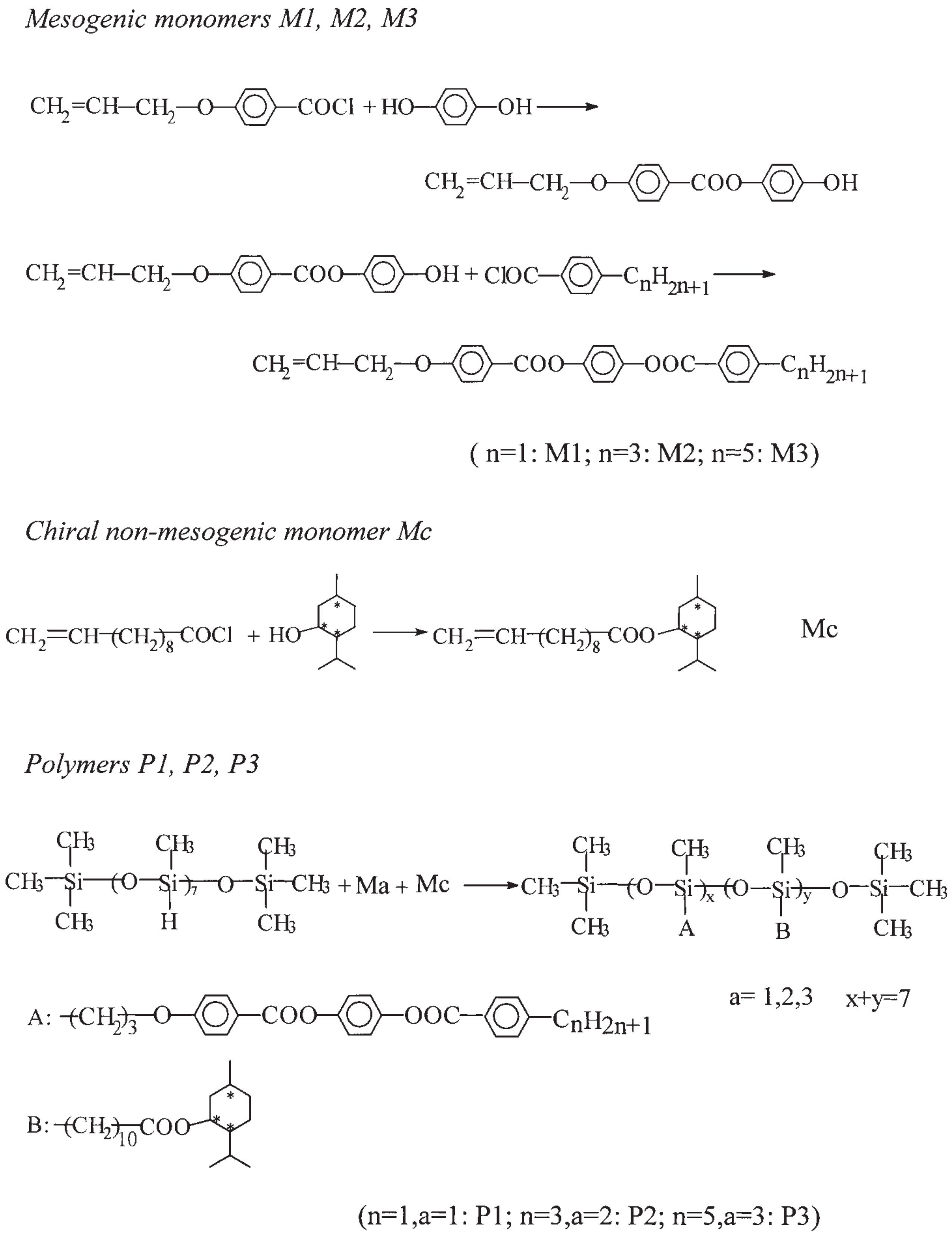

Scheme. Synthesis of monomers and polymers.

Table 2. Polymerization and thermal analysis results for polymers P1, P2, P3.

	Feed/mmol			Thermal results							
Polymer	PMHS/M1/ Mc	Mc[a]	$-[\alpha]_D^{15}$	T_g/ °C	T_1/ °C	T_i/ °C	ΔH_i/ J g^{-1}	ΔT^b/ °C	$T_c{}^c$/ °C	ΔH_c/ J g^{-1}	$T_{5\%}{}^d$/ °C
$P1_0$	1/7.00/0.00	0.0	—	55.4	—	250.4	2.25	195.0	242.5	1.11	358.2
$P1_1$	1/6.65/0.35	5.0	—	56.3	—	232.1	1.98	175.8	224.9	1.02	330.8
$P1_2$	1/6.30/0.70	10.0	—	49.4	—	216.3	1.26	165.1	207.2	0.88	329.0
$P1_3$	1/5.95/1.05	15.0	—	43.2	—	192.8	0.71	149.6	183.2	0.49	344.5
$P1_4$	1/5.60/1.40	20.0	4.4	42.2	—	171.6	0.98	129.4	161.7	0.36	310.5
$P1_5$	1/4.90/2.10	30.0	5.8	35.8	70.8	131.8	1.01	96.0	—	—	302.8
$P1_6$	1/4.20/2.80	40.0	7.6	34.3	67.1	101.8	0.43	67.5	—	—	326.3
$P1_7$	1/3.50/3.50	50.0	9.3	—	—	55.5	2.78	—	—	—	304.2
$P2_0$	1/7.00/0.00	0.0	—	49.0	—	235.8	1.95	186.8	231.2	1.58	358.0
$P2_1$	1/6.65/0.35	5.0	—	48.2	—	221.6	1.95	173.4	215.1	1.43	342.5
$P2_2$	1/6.30/0.70	10.0	3.9	47.3	—	203.3	1.30	156.0	199.6	0.78	333.8
$P2_3$	1/5.95/1.05	15.0	4.8	45.5	—	184.2	0.78	138.7	182.0	0.64	311.4
$P2_4$	1/5.60/1.40	20.0	6.4	40.1	—	168.4	0.92	128.3	165.1	0.66	313.0
$P2_5$	1/4.90/2.10	30.0	8.0	33.0	72.0	135.5	0.68	102.5	—	—	309.3
$P2_6$	1/4.20/2.80	40.0	9.9	42.2	66.8	101.0	—	58.8	—	—	315.5
$P2_7$	1/3.50/3.50	50.0	12.1	43.3	63.7	—	—	—	—	—	326.2
$P3_0$	1/7.00/0.00	0.0	—	46.8	68.3	225.3	1.35	178.5	210.4	1.01	350.8
$P3_1$	1/6.65/0.35	5.0	—	44.9	68.1	210.3	1.48	165.4	204.2	0.60	343.2
$P3_2$	1/6.30/0.70	10.0	4.6	44.2	—	194.8	1.70	150.6	181.0	0.38	327.9
$P3_3$	1/5.95/1.05	15.0	5.9	43.0	70.7	181.5	1.11	138.5	173.0	1.20	334.2
$P3_4$	1/5.60/1.40	20.0	6.8	40.1	68.4	167.2	1.55	127.1	155.5	0.37	337.1
$P3_5$	1/4.90/2.10	30.0	7.9	38.4	65.8	135.3	0.26	96.9	130.5	0.45	316.9
$P3_6$	1/4.20/2.80	40.0	9.2	37.0	63.7	105.8	0.96	68.8	—	—	325.1
$P3_7$	1/3.50/3.50	50.0	10.8	35.9	47.4	—	—	—	—	—	334.4

[a] Mol% of Mc based on M1, or M2, or M3 + Mc.
[b] The mesomorphic temperature range (T_i–T_g).
[c] Transition temperature and enthalpy from isotropic to mesomorphic phase in cooling.
[d] Temperature at which 5% loss occurred.

density of optically active centres per mass of polymer sample as the Mc content increased in the grafting copolymerization reactions.

3.2. *Liquid crystal behaviour of monomers M1–M3*

The LC properties of monomers M1–M3 were characterized by differential scanning calorimetry (DSC) and polarizing optical microscopy (POM). The phase transition temperatures of monomers are summarized in table 1; the representative DSC thermograms are shown in figure 2(*a*). The heating and cooling thermograms of the monomers contained two phase transition endotherms and exotherms, respectively. In the heating thermograms, the first endotherm indicated the transition from solid to mesomorphic phase at temperature T_m; the second endotherm showed the transition from mesogenic to isotropic phase (T_i). In the cooling thermograms, the first exotherm showed the transition from isotropic to mesomorphic phase (T_c); the second corresponded to crystallization (T_{cr}). T_m, T_i, T_c and T_{cr} decreased on going from M1 to M3 (table 1), due to the increase in flexibility of molecular chains for the terminal group changing from methyl, *n*-propyl to *n*-amyl. The mesomorphic temperature ranges of the monomers (Δ *T* and Δ *T*') were wider than 100°C. Monomers M1, M2, M3 exhibited typical nematic threadlike textures when being heated to above T_m, The textures were unchanged up to T_i when observed by POM; the same nematic threadlike textures were observed on cooling, [see figure 5(*a*)], which indicated that monomers M1, M2 and M3 exhibited enantiotropic nematic mesophases.

3.3. *Liquid crystalline behaviour of the polymers*

The thermal behaviour of all the polymers synthesized are summarized in table 2; representative DSC thermograms are given in figure 2(*b*). Transition temperatures are plotted against the Mc content in figure 3.

The glass transition temperature (T_g) is an important parameter in connection with the structure and properties of the polymers. The polymeric chain flexibility, molecular mass, mesogenic group and length of the

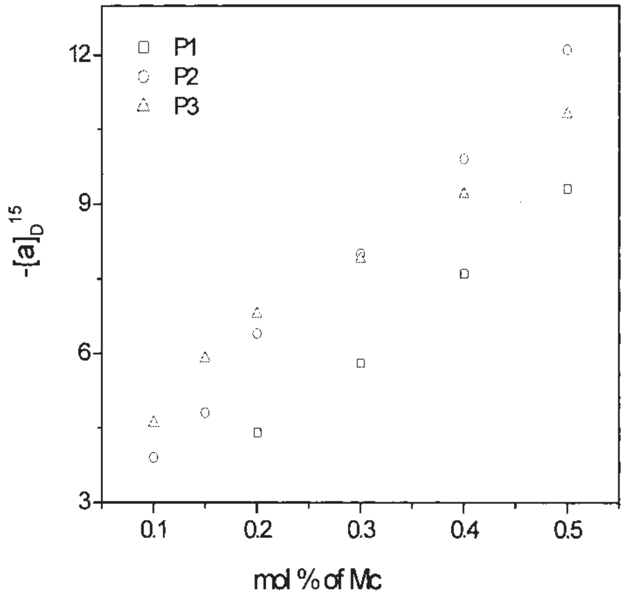

Figure 1. Variation of SRP with concentration of Mc in the polymers.

flexible spacer influence the T_g value of the side chain LCPs. The T_g of polymers P1, P2 and P3 ranged from 30 to 55°C, and decreased with increasing concentration of chiral monomer. The decrease of T_g was mainly due to the decrease in the content of rigid mesogenic units, thus increasing the flexibility of the polymers. Polymer T_g is also influenced by the steric effect of the menthyl group. Compared with $P1_0$, the T_g of $P2_0$ decreased by 6.4°C, while the T_g of $P3_0$ decreased by 8.6°C (table 2). Polymers $P1_0$, $P2_0$ and $P3_0$ contain only the rod-like mesogenic monomer, and their aliphatic terminal groups are methyl, *n*-propyl and *n*-amyl, respectively. The flexibility increases from M1 to M3, so T_g decreases on going from $P1_0$ to $P3_0$.

The clearing point (T_i) was influenced by the flexibility of polymer molecules, the steric effect of large groups and the concentration of mesogenic units. The T_i decreased with increasing the concentration of Mc. This was mainly due to the increase in flexibility of the polymers, which would reduce the energy of disorientation of polymer molecules in the LC phase. The decrease in concentration of mesogenic units and the steric effect of the menthyl group both influenced the T_i. The mesomorphic temperature range (Δ T) of the polymers varied systematically with the change of T_g and T_i. The graphical trends of Δ T values were found to be identical when varied with the content of Mc for P1, P2 and P3, in figure 4. The mesomorphic temperature ranges of the polymers were wider than 100°C. The transition temperature (T_c) from isotropic to mesomorphic phase on cooling decreased with decreasing content of mesogenic units; this corresponds to the inverse process of phase transition of T_i. The phase transition temperature T_1, which is little higher than T_g, corresponded to the movement of the whole molecular chain, or of the longer chain segments in the amorphous polymers. X-ray analysis showed that P1, P2 and P3 were amorphous. The $T_{5\%}$ of all the polymers were over 300°C in a N_2 atmosphere.

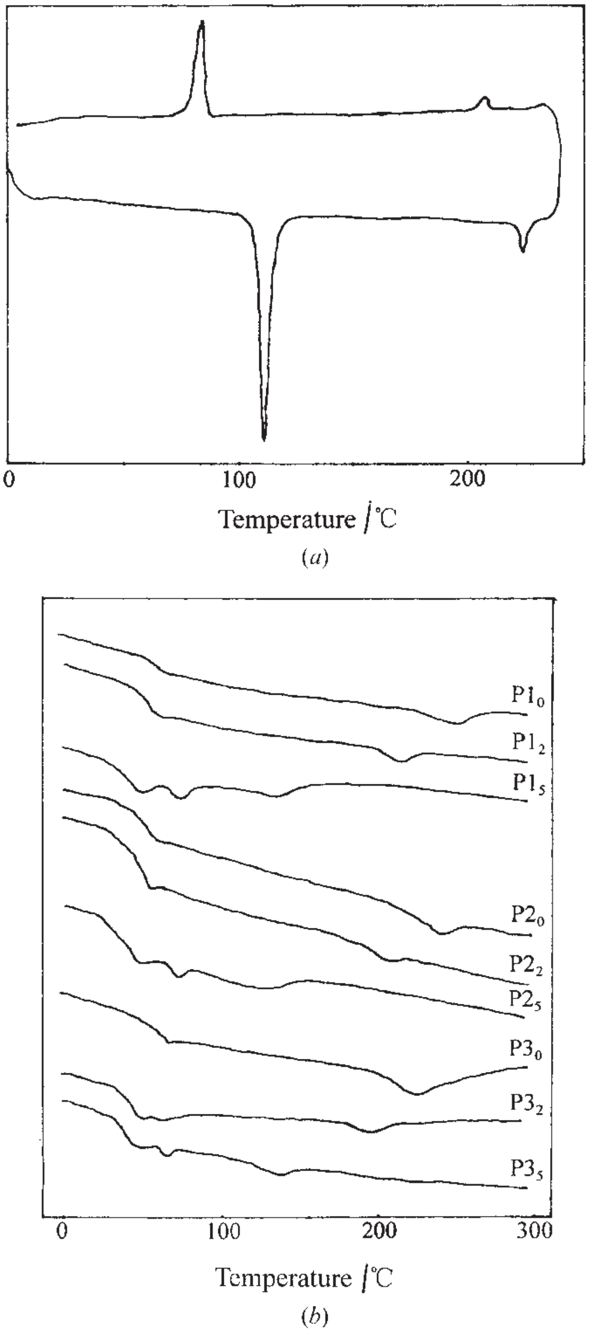

(*a*)

(*b*)

Figure 2. DSC thermograms of monomer and polymers: (*a*) monomer M3; (*b*) polymers on heating.

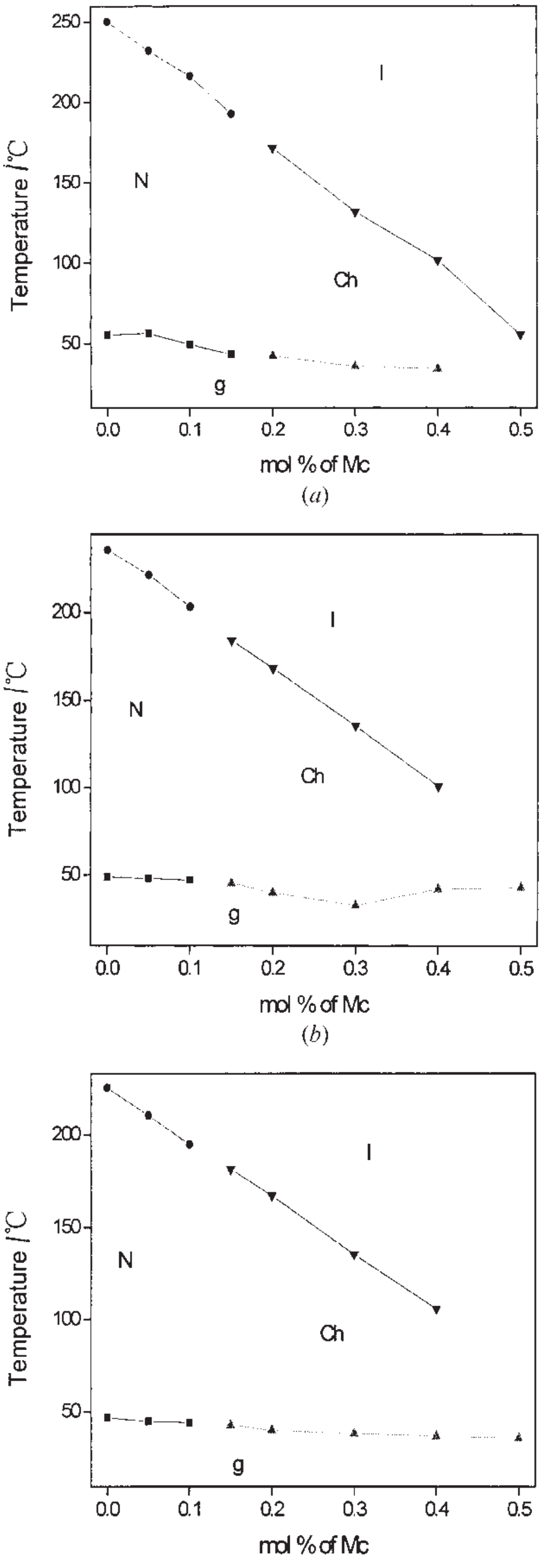

(*a*)

(*b*)

(*c*)

Figure 3. Phase transition temperatures of polymers as a function of Mc concentration. (I: isotropic; N: nematic; Ch: cholesteric; g: glass). (*a*) P1 series, (*b*) P2 series, (*c*) P3 series.

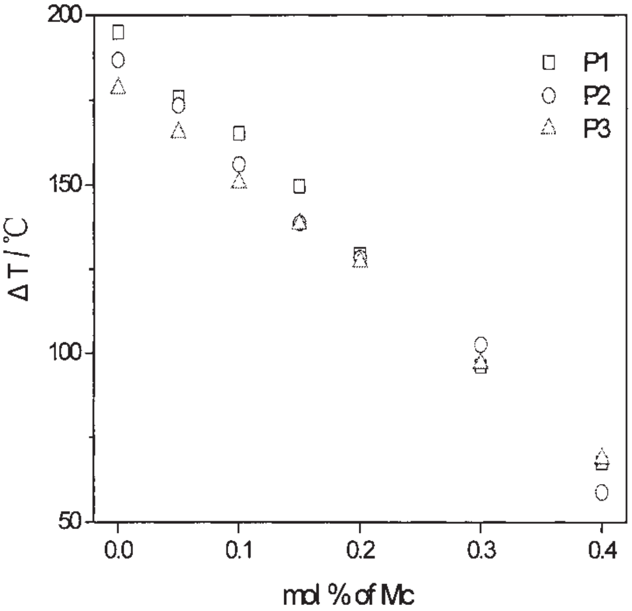

Figure 4. Δ T of polymers as a function of Mc concentration.

All the polymers displayed a thermotropic mesophase, and exhibited different colourful textures when observed under POM. Transition temperatures obtained by POM agreed with thermal data gained from DSC (which were within ± 10°C because of the effects of superheating and supercooling) [5]. The polymers exhibited clear threadlike textures, figure 5(*b*), on heating; the same textures were observed on cooling when the content of the chiral non-mesogenic unit was lower than 10 mol% for polymers P2 and P3 and 15 mol% for polymers P1. The typical nematic threadlike textures were attributed to the line-disclinations of the nematic mesophase. The polymer molecules aligned with helix structures, because the intensity of chiral centres increased to some degree. Defects that would produce different textures, included not only line-disclinations, but also whorl-dislocations and whorl-dispirations; the polymers displayed multiple colourful textures, which were different from the nematic threadlike textures. Figure 5(*c*) shows the Grand-Jean texture of polymer $P1_4$, together with a few threadlike textures. For $P1_4$, the defects included line-disclinations, whorl-dislocations and whorl-dispirations because the concentration of chiral units was only 20 mol%; the line-disclinations produced the threadlike textures. The increase in chiral units led to whorl-dislocations and whorl-dispirations produced by helix structures; the resulting colourful Grand-Jean textures are shown in figure 5(*d*).

XRD patterns of quenched polymer samples are shown in figure 6. The data were collected in two 2θ ranges, $2\theta = 0.2°–5°$ and $5°–60°$, with different divergence and receiving slits being used in the two ranges. In all the

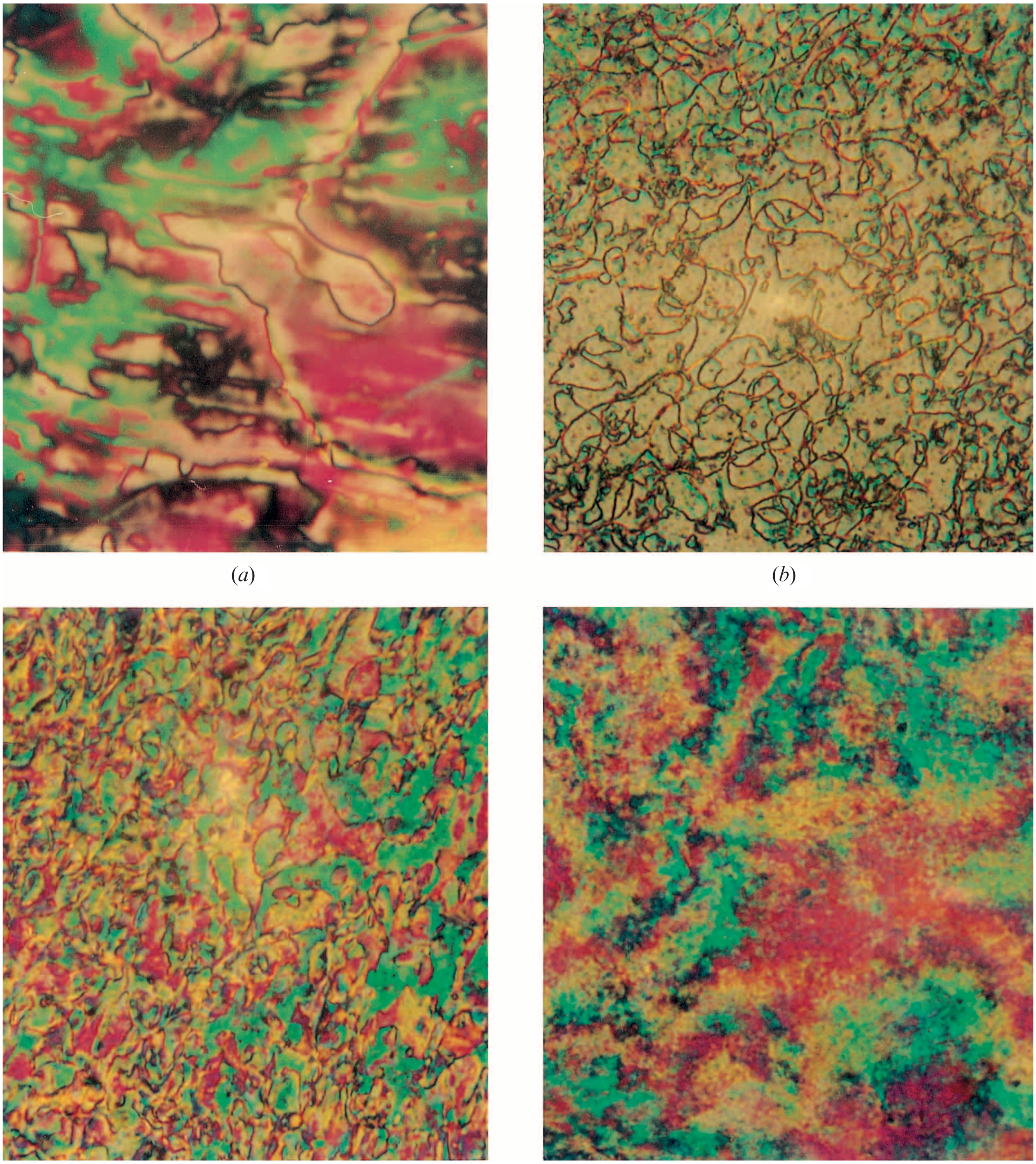

Figure 5. Polarizing optical micrographs (200 ×) of mesogenic monomer and polymers. (*a*) M3 at 217.5°C; (*b*) $P2_1$ at 167.1°C; (*c*) $P1_4$ at 155.5°C; (d) $P3_6$ at 86.6°C.

patterns recorded there were weak and strong diffuse diffraction maxima occurring at $2\theta = 10.0°–11.0°$ (weak) and $2\theta = 19.0°–20.5°$ (strong) in the wide range diffraction angle. This was evidence of the polymers amorphous nature. The $d1 = 0.884–0.804$ nm ($2\theta = 10.0°–11.0°$) and $d2 = 0.467–0.433$ nm ($2\theta = 19.0°–20.5°$), obtained from the 2θ values and the Bragg equation, corresponded to the lateral distances between molecules; this was the intermolecular distance perpendicular to the molecular long axes. No sharp Bragg reflections were observed for polymers in the lower angle regions ($2\theta < 5°$), which indicated that the constituent molecules of the polymers did not regularly arrange within the two-dimensional order structure as a smectic mesophase [16].

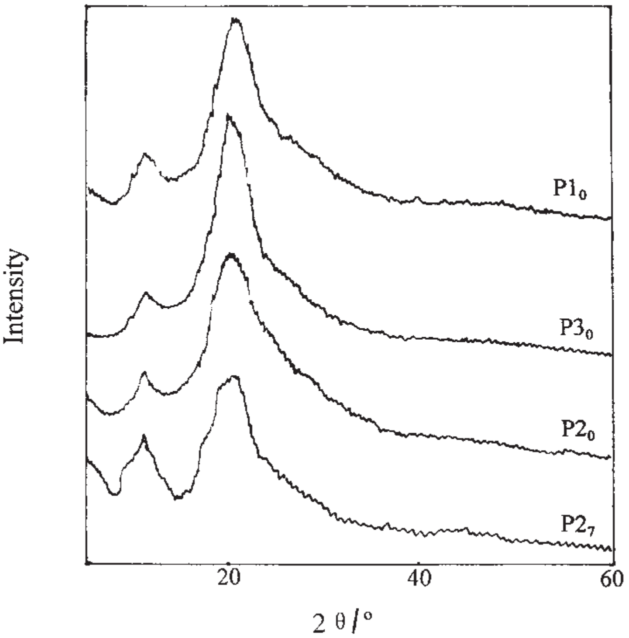

Figure 6. X-ray patterns of the polymers.

4. Conclusion

Thermotropic liquid crystalline polymers ($P1_0$–$P1_7$, $P2_0$–$P2_7$ and $P3_0$–$P3_7$), containing mesogenic units with different flexible terminal groups and a chiral unit with a chiral menthyl group, were synthesized by grafting upon a polysiloxane backbone. All the polymers exhibited thermotropic liquid crystalline properties over a wide (100°C) mesogenic region. The polymers exhibited typical colourful cholesteric Grand-Jean textures when the content of the chiral non-mesogenic unit was higher than 15 mol% for polymers P1, and higher than 10 mol% for polymers P2 and P3. The other polymers exhibited typical nematic threadlike textures. Most of the polymers were laevorotatory and their SRPs increased with increasing content of chiral units. All of the polymers were thermally stable over 300°C.

The authors are grateful to the National Natural Scientific Fundamental Committee of China, and National Basic Research Priorities of China, for financial support of this work.

References

[1] Donald, A. M., and Windle, A. H., 1994, *Liquid Crystalline Polymers* (Cambridge: Cambridge University Press).
[2] Zhao, L., He, C. B., and Chung, T. S., 2001, *J. polym. Sci. A: polym. Chem.*, **39**, 1288.
[3] Meyer, R. B., Liebert, L., Strezeleki, L., and Keller, P., 1975, *J Phys. (Paris)*, **36**, L69.
[4] Decobert, G., Duboid, J. C., Esselin, S., and Noel, C., 1986, *Liq. Cryst.*, **1**, 307.
[5] Rukmani, S., and Ganga, R., 2001, *J polym. Sci. A: polym. Chem.*, **39**, 1743.
[6] Mastrangelo, J. C., and Chen, S. H., 1993, *Macromolecules*, **26**, 6132.
[7] Takashi, M., Kazuhiro, N., and Keisuke, F., 1997, *Polym. J.*, **29**, 309.
[8] Huai, Y., and Hirotsugu, K., 2002, *Liq. Cryst.*, **29**, 1141.
[9] Natarajan, L. V., Bunning, T. J., and Kim, S. Y., 1994, *Macromolecules*, **27**, 7248.
[10] Hu, J. S., Zhang, B. Y., Liu, Z. J., and Zang, B. L., 2001, *J appl. polym. Sci.*, **80**, 2335.
[11] Zhi, J. G., Zhang, B. Y., and Zang, B. L., *et al*, *J. appl. polym. Sci.* (to be published).
[12] Zhi, J. G., Zhang, B. Y., Zang, B. L., and Dou, Z., 2002, *Northeastern University (Natural Science)*, 23, 606.
[13] Altomare, A., Carlini, C., and Panattoni, M., 1984, *Macromolcules*, **17**, 2207.
[14] Cabrera, I., Krongauz, V., and Ringsdorf, H., 1988, *Mol. Cryst. liq. Cryst.*, **155**, 221.
[15] Van't hoff, J. H., 1894, *Dielagerung der Atome im Raum*, 2nd Edn (Braunschweig; Vieweg), p. 119.
[16] Liang, X. X., Zhang, L. Z., and Wang, J., *et al*, 2001, *Acta Polym Sinica*, 109.